Deep Neural Network for Foreign Object Detection in Chest X-rays

*K.C. Santosh, Senior Member, *IEEE*, Mrinal K Dhar, Ramina Rajbhandari, Amul Neupane
Department of Computer Science, The University of South Dakota
414 E Clark St, Vermillion, SD 57069, USA
santosh.kc@ieee.org (*corr. author) and {mrinal.dhar, amul.neupane, ramina.rajbhandari}@coyotoes.usd.edu

***Abstract*—In automated Chest X-Ray (CXR) screening process, foreign objects, such as coins/buttons, medical tubes and devices, and jewelries can adversely impact the performance. In an automated process, conventional machine learning algorithms did not separately consider them into account, and as a consequence, they results in false positive cases. In this paper, we address the use of Deep Neural Network (DNN) to detect circle-like foreign objects of difference sizes in CXRs. We present faster Region-based Convolutional Neural Network (R-CNN) for foreign object detection on a set of 400 publicly available CXR images hosted by LHNCBC, U.S. National Library of Medicine (NLM), National Institutes of Health (NIH). The proposed DNN achieved 97% precision, 90% recall, and 93% F1-score. The results are comparable with the existing techniques.**

***Index Terms*—Deep Neural Networks, Faster R-CNN, Foreign Objects, Tuberculosis, Chest X-Rays.**

I. Introduction

Along several lung diseases, such as Pneumonia, lung cancer, and pulmonary edema, Tuberculosis (TB) is still considered as a major health threat across the world [1], In this report, it stated that 7 million people have received record levels of lifesaving TB treatment and other 3 million were still missed out. In this context, tools are techniques that are based on Artificial Intelligence (AI) could be of great help/support when we consider mass screening. Most of the AI-driven tools used radiological image data, since it carries more information than other data types. Clinical studies suggested that TB manifestations are well observed in Chest X-Ray (CXR) and therefore, CXR has been widely used for a long decades since 60's. For any automated CXR screening tool, abnormalities can be analyzed through Anomaly Detection (AD) techniques. AD tools/techniques help find/identify rare/unusual observations that bring suspicions by differing significantly from the majority of the data or with respect to a set of normal data.

More often, instead of using AD-based tools, in CXR screening tools follows conventional train, validate, and test case scenarios [2]–[5]. These machine learning algorithms typically employ handcrafted features from CXRs without taking separately foreign objects into account. As a consequence, the presence of foreign objects in CXRs impacts the overall performance of the specific AI-driven tool. The exact similar impact is observed in deep learning-based models, where the primary idea is just to avoid feature engineering. For example, from our prior works [2]–[7], we observe that in CXR images, foreign objects, such as coins/buttons (see Fig 1), cardiac pacemakers, and other medical devices result in CXR screening errors due to algorithms confusing them with similar appearing pulmonary abnormalities [8]–[10]. In other words, to build a successful abnormality screening tool, it is wise to consider detecting and/localizing foreign objects in CXRs. Avoiding them while training AI-driven abnormality screening tool helps improve the performance by reducing possible false positives.

Detecting and localizing the foreign objects in CXRs are not trivial [11], [12]. Foreign object detection in CXRs does not rich state-of-the-art literature. In general, state-of-the-art techniques used basic image processing and pattern recognition techniques, such as Viola-Jones, circular Hough transform (CHT), and candidate selection (CS) plus CHT to locate circular elements in CXRs. Later in 2018, Zohora et al [13] introduced a fully machine learning-based technique, where authors used normalized cross-correlation using a few templates to collect potential circle-like elements and unsupervised clustering to make a decision. Unlike previous approaches, Zohora et al does not heavily rely on changes in image intensity values.

Instead of relying on handcrafted features for object detection, it is important to let machine decides their discriminant features in accordance with the objective i.e., foreign objects in our study. The use of deep learning idea inherently supports variation/change in dataset in size over time. Further, regional variations do not negatively influence the performance of the tool. With this concept, in this paper, we proposed faster region-based convolutional neural networks (R-CNN) to detect circle-like foreign elements (see Fig. 1) in CXR images that helps avoid confusions in CXR screening for the evidence of abnormalities, such as nodules and other calcifications. We validated the proposed tool on a set of 400 publicly available images hosted by LHNCBC, U.S. National Library of Medicine (NLM), National Institutes of Health (NIH). In our learning/training process, we aimed at reducing the error rates minimum possible; technically, 10^{-4}. Localizing their spatial position in CXR helps further avoid possible confusions during the abnormality screening process.

The structure of the paper can be summarized as follows. In Section II, we discuss faster R-CNN architecture for foreign object detection. In Section III, we include experimental set up, protocol, and results. The latter of the section includes analysis of the results (with comparison). In Section IV, we

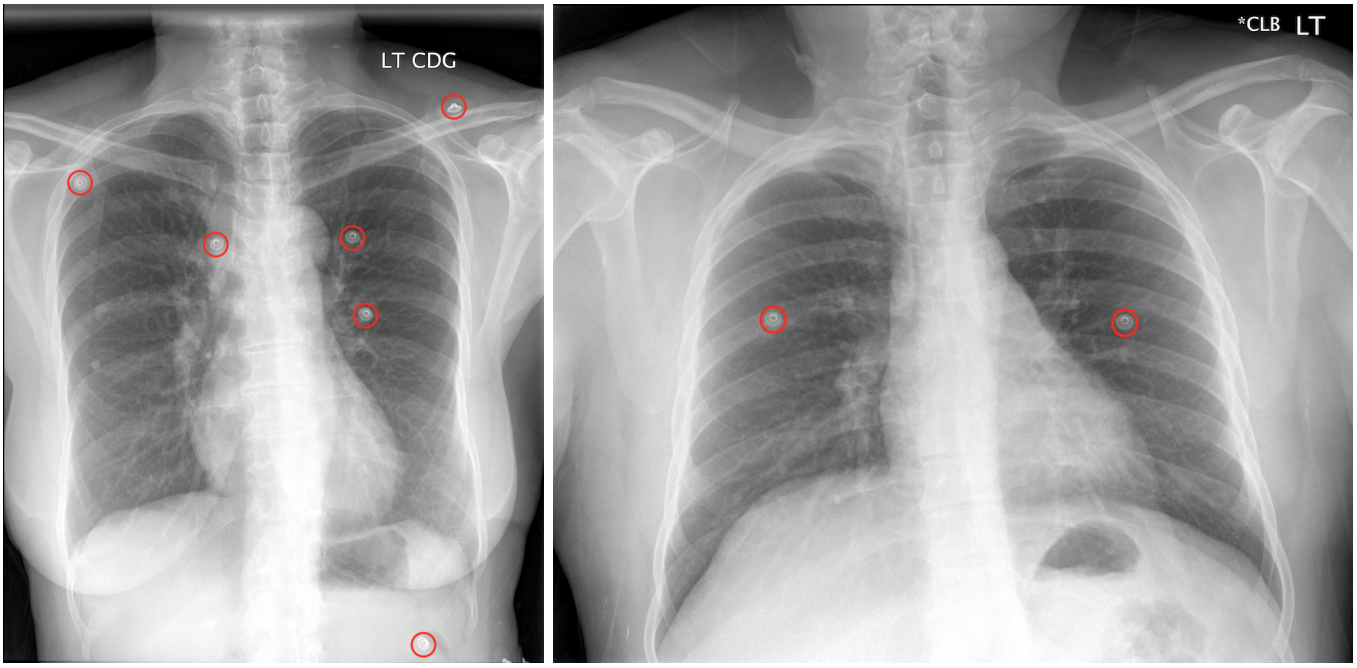

Fig. 1. Illustrating circle-like foreign objects in CXR (annotating in red). They are, somehow, similar to lung abnormalities, like nodules.

conclude the paper.

II. Deep Neural Network (faster R-CNN) for foreign object detection in CXR

Detecting objects using only a standard Convolutional Neural Network (CNN) (followed by a Fully Connected (FC) layer is not always efficient. The primary reason behind this is, we do not have prior information about Regions-Of-Interest (ROIs), representing foreign objects in the image. This varies the length of the output layer. In [14], Girshick et al. proposed a method R-CNN, where they extracted 2000 regions (using selective search algorithm), which they called region proposals. A CNN was then applied to extract features that were fed to Support Vector Machine (SVM) for classification purpose. The problem with the R-CNN is that it suffers from heavy computational time during training testing 2000 region proposals per image. Fast R-CNN [15], on the other hand, instead of using 2000 region proposal to the CNN per image, it uses the original images to the CNN only once, and generates convolutional feature maps from which it identifies the region proposals using selective search. However, the selective search affects network performance as it is computationally expensive. In faster R-CNN [16], the input images are passed through a pre-trained convolutional neural network (CNN). This CNN acts as a feature extractor. Once the feature map is obtained, a separate convolutional network is used on it to predict the region proposals. This network is called Region Proposal Network (RPN). Note that, at this point, fast R-CNN used selective search algorithm on the feature map to find out region proposals. Faster R-CNN replaces selective search algorithm with RPN. RPN is used to find out a predefined number of regions or bounding boxes that may have objects in it. Anchor boxes are used to capture the scale and aspect ratio of the class that we want to detect. The size of the anchor boxes is generally chosen based on the object sizes in the training data. Now that we have the feature maps and the bounding boxes containing the relevant objects, we simply extract the desired features by using ROI pooling. Finally, the R-CNN module classifies the object in the bounding box and adjusts the coordinates of the bounding box to fit the object better. Softmax function is used to predict the object's class, while a regression layer is to help localize the bounding boxes.

In short, the following is the architecture (Fig. 2), we implemented in our study. Simply, we have three sections: input, middle, and output.

1) Input data is fed in the input section.
2) The middle section contains three repeated blocks of convolutional, Rectified Linear Unit (ReLU), and pooling layers. The first two convolution layers used 32 filters while 64 for the last one. The filter size, stride, and padding are set to 5×5, 1, and 2, respectively. All the pooling layers have 3×3 filters.
3) The output section consists of five layers: FC layer with 64 neurons, ReLU, FC layer with 10 neurons, Softmax loss layer, and classification layer (using Cross Entropy). For optimization, we used Stochastic gradient descent with momentum (SGDM) optimizer.

III. Experiments

This section includes a) dataset collection; b) evaluation metrics; and c) results and comparative studies. In what follows, we consider them one after another.

1) Dataset collection:

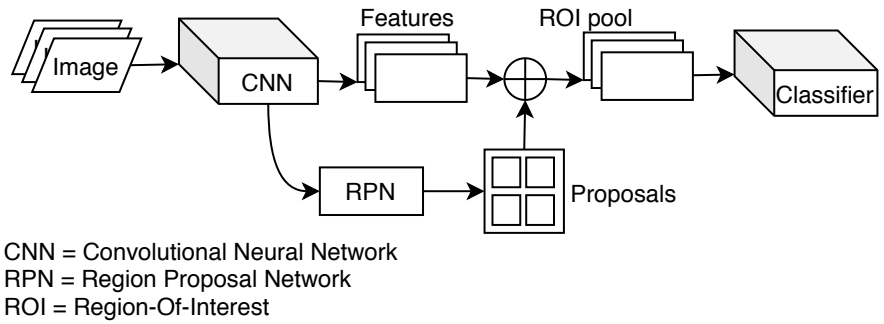

Fig. 2. Faster R-CNN: workflow.

For a fair comparison, like in the previous works, we used 400 CXRs from the Indiana CXR dataset maintained by U.S. National Library of Medicine (NLM), National Institutes of Health (NIH). In 400 CXRs, there are 1178 circle-like objects, where 325 of them are within the lung region.

2) Metrics:
To measure how well the proposed tool works, the following metrics:
a) Precision (P = TP/(TP+FP));
b) Recall (R =TP/(TP+FN)); and
c) F1 score (F1 = 2×((P×R)/(P+R)),
where TP, FP, and FN refer to True Positive, False Positive, and False Negative, respectively.

3) Results and analysis:
We experimented on two different set ups: a) Without Lung Segmentation (WoLS); and b) With Lung Segmentation (WLS). As pulmonary abnormalities lie within the lung regions/sections, it is fair to focus on results that are received after lung segmentation [17].
In our test, we used 175 CXRs for training and remaining 225 CXRs for testing. In Table I, the test performance scores are provided.
We compared our method with four other techniques that were recently reported in the literature [11], [13], [18]: Viola-Jones, CHT, candidate selection followed by CHT (CS + CHT), and normalized correlation and unsupervised clustering. Comparative studies are provided in Tables II and III. Of all, the proposed tool performs the best. Using WLS experimental set up, the proposed tool is better than the best of all (from the literature) by 7% in precision and 2% in F1 score. The results, for better understanding, are provided in Fig. 3.

TABLE I
OUR RESULTS (SCORES ARE IN %): WOLS AND WLS.

	Precision	Recall	F1 Score
WoLS	0.91	0.92	0.91
WLS	0.97	0.9	0.93

Index:
WoLS = Without Lung Segmentation
WLS = With Lung Segmentation

TABLE II
COMPARISON (SCORES ARE IN %): WITHOUT LUNG SEGMENTATION (WOLS)

Method	Precision	Recall	F1 Score
Xue et al. (Voila-Jones) [11]	0.37	0.94	0.53
Xue et al. (CHT) [11]	0.81	0.45	0.58
Zohora et al. (CS + CHT) [18]	0.85	0.54	0.66
Zohora et al. (Normalized Correlation + Unsupervised Clustering) [13]	0.76	0.88	0.81
DNN (Proposed Tool)	0.906	0.92	0.913

TABLE III
COMPARISON (SCORES ARE IN %): WITH LUNG SEGMENTATION (WLS)

Method	Precision	Recall	F1 Score
Xue et al. (Voila-Jones) [11]	0.36	1	0.52
Xue et al. (CHT) [11]	0.94	0.74	0.83
Zohora et al. (CS + CHT) [18]	0.96	0.90	0.92
Zohora et al. (Normalized Correlation + Unsupervised Clustering) [13]	0.90	0.93	0.91
DNN (Proposed Tool)	0.97	0.90	0.93

IV. CONCLUSION

In this work, we have employed a Deep Neural Network (faster Region-based Convolutional Neural Network (R-CNN)) to detect circle-like foreign objects in chest X-Rays. We have validated the use of the proposed DNN on a set of 400 publicly available CXR images hosted by LHNCBC, U.S. National Library of Medicine (NLM), National Institutes of Health (NIH), and have achieved 97% precision, 90% recall, and 93% F1-score. The results outperformed the state-of-the-art techniques.

The immediate plan is to check whether localizing/avoiding circle-like foreign objects, such as coins and buttons can help improve the performance of the abnormality screening, as they can be considered as nodules, and nodule is one of the primary indicators of TB.

ACKNOWLEDGMENTS

Authors would like to acknowledge two grants titled a) 'Advanced body screening at the Airport using Deep Learning' (FY2019) and b) 'Deep Medical Imaging for Foreign

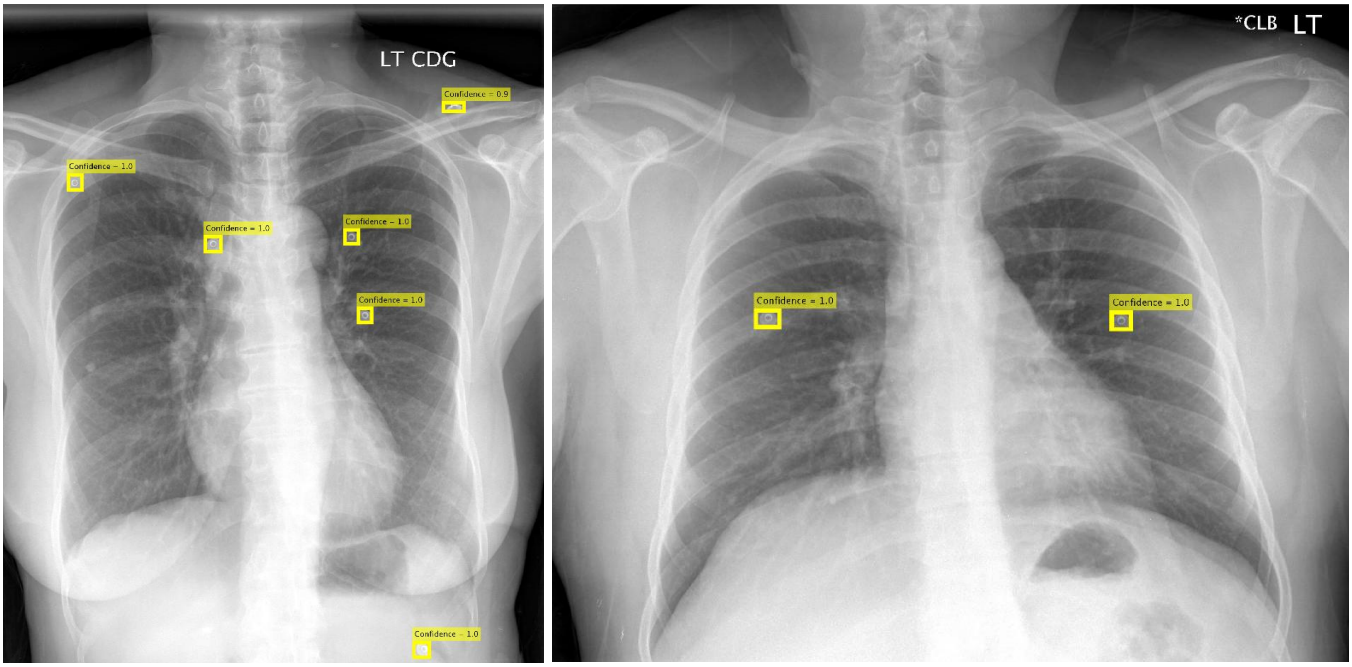

Fig. 3. Automatic circle-like foreign object detection (with confidence score) using the faster R-CNN (*cf.* Fig. 1).

Object Detection in Chest Radiographs' (F2020) received from Graduate Research & Creative Scholarship Grants, Graduate School, The University of South Dakota.

REFERENCES

[1] WHO, "World health organization, global tuberculosis report," 2019.

[2] K. C. Santosh, S. Vajda, S. Antani, and G. R. Thoma, "Edge map analysis in chest x-rays for automatic pulmonary abnormality screening," *International journal of computer assisted radiology and surgery*, pp. 1–10, 2016.

[3] A. Karargyris, J. Siegelman, D. Tzortzis, S. Jaeger, S. Candemir, Z. Xue, K. C. Santosh, S. Vajda, S. Antani, L. Folio, *et al.*, "Combination of texture and shape features to detect pulmonary abnormalities in digital chest x-rays," *International journal of computer assisted radiology and surgery*, vol. 11, no. 1, pp. 99–106, 2016.

[4] M. Ding, S. Antani, S. Jaeger, Z. Xue, S. Candemir, M. Kohli, and G. Thoma, "Local-global classifier fusion for screening chest radiographs," 2017.

[5] K. C. Santosh and S. Antani, "Automated chest x-ray screening: Can lung region symmetry help detect pulmonary abnormalities?," *IEEE Transactions on Medical Imaging*, vol. PP, no. 99, pp. 1–1, 2017.

[6] K. C. Santosh, S. Vajda, S. K. Antani, and G. R. Thoma, "Automatic pulmonary abnormality screening using thoracic edge map," in *28th IEEE International Symposium on Computer-Based Medical Systems, CBMS 2015, Sao Carlos, Brazil, June 22-25, 2015*, pp. 360–361, 2015.

[7] S. Vajda, A. Karargyris, S. Jäger, K. C. Santosh, S. Candemir, Z. Xue, S. K. Antani, and G. R. Thoma, "Feature selection for automatic tuberculosis screening in frontal chest radiographs," *J. Medical Systems*, vol. 42, no. 8, pp. 146:1–146:11, 2018.

[8] S. Sakai, H. Soeda, N. Takahashi, T. Okafuji, T. Yoshitake, H. Yabuuchi, I. Yoshino, K. Yamamoto, H. Honda, and K. Doi, "Computer-aided nodule detection on digital chest radiography: Validation test on consecutive T1 cases of resectable lung cancer," *J. Digital Imaging*, vol. 19, no. 4, pp. 376–382, 2006.

[9] G. Simk, G. Orbn, P. Mday, and G. Horvth, "Elimination of clavicle shadows to help automatic lung nodule detection on chest radiographs," in *European Conference of the International Federation for Medical and Biological Engineering* (J. Sloten, P. Verdonck, M. Nyssen, and J. Haueisen, eds.), vol. 22, pp. 488–491, Springer Berlin Heidelberg, 2009.

[10] M. T. Freedman, S.-C. B. Lo, J. C. Seibel, and C. M. Bromley, "Lung nodules: Improved detection with software that suppresses the rib and clavicle on chest radiographs," *Radiology*, vol. 260, no. 1, pp. 265–273, 2011.

[11] Z. Xue, S. Candemir, S. Antani, L. R. Long, S. Jaeger, D. Demner-Fushman, and G. R. Thoma, "Foreign object detection in chest x-rays," in *Bioinformatics and Biomedicine (BIBM), 2015 IEEE International Conference on*, pp. 956–961, IEEE, 2015.

[12] F. T. Zohora and K. C. Santosh, "Foreign circular element detection in chest x-rays for effective automated pulmonary abnormality screening," pp. 36–49, 2017.

[13] F. T. Zohora, S. K. Antani, and K. C. Santosh, "Circle-like foreign element detection in chest x-rays using normalized cross-correlation and unsupervised clustering," in *Medical Imaging 2018: Image Processing, Houston, Texas, United States, 10-15 February 2018*, p. 105741V, 2018.

[14] R. Girshick, J. Donahue, T. Darrell, and J. Malik, "Rich feature hierarchies for accurate object detection and semantic segmentation," in *2014 IEEE Conference on Computer Vision and Pattern Recognition*, pp. 580–587, 2014.

[15] R. B. Girshick, "Fast R-CNN," *CoRR*, vol. abs/1504.08083, 2015.

[16] S. Ren, K. He, R. Girshick, and J. Sun, "Faster r-cnn: Towards real-time object detection with region proposal networks," *IEEE Transactions on Pattern Analysis and Machine Intelligence*, vol. 39, no. 6, pp. 1137–1149, 2017.

[17] S. Candemir, S. Jaeger, K. Palaniappan, J. P. Musco, R. K. Singh, Z. Xue, A. Karargyris, S. Antani, G. Thoma, and C. J. McDonald, "Lung segmentation in chest radiographs using anatomical atlases with nonrigid registration," *IEEE transactions on medical imaging*, vol. 33, no. 2, pp. 577–590, 2014.

[18] F. T. Zohora and K. C. Santosh, "Circular foreign object detection in chest x-ray images," in *International Conference on Recent Trends in Image Processing and Pattern Recognition*, pp. 391–401, Springer, 2016.